Plant Communications
Research article

CellPress
Partner Journal

Microbe-induced coordination of plant iron–sulfur metabolism enhances high-light-stress tolerance of *Arabidopsis*

Kirti Shekhawat[1], Alaguraj Veluchamy[2], Anam Fatima[1], Gabriel X. García-Ramírez[1,3], Jean-Philippe Reichheld[4,5], Olga Artyukh[1], Katja Fröhlich[1], Alexander Polussa[6], Sabiha Parween[1], Arun Prasanna Nagarajan[1], Naganand Rayapuram[1] and Heribert Hirt[1,*]

[1]Biological and Environmental Sciences and Engineering Division, King Abdullah University of Science and Technology (KAUST), 23955-6900 Thuwal, Saudi Arabia

[2]Department of Computational Biology, St. Jude Children's Research Hospital, Danny Thomas Place, Memphis, TN 38105, USA

[3]Max Planck Institute for Plant Breeding Research, 50829 Cologne, Germany

[4]Laboratoire Génome et Développement des Plantes, Université Perpignan Via Domitia, 66860 Perpignan, France

[5]Laboratoire Génome et Développement des Plantes, CNRS, 66860 Perpignan, France

[6]The Forest School, Yale School of the Environment, Yale University, New Haven, CT 06520, USA

***Correspondence: Heribert Hirt (heribert.hirt@kaust.edu.sa)**

https://doi.org/10.1016/j.xplc.2024.101012

ABSTRACT

High-light stress strongly limits agricultural production in subtropical and tropical regions owing to photo-oxidative damage, decreased growth, and decreased yield. Here, we investigated whether beneficial microbes can protect plants under high-light stress. We found that *Enterobacter* sp. SA187 (SA187) supports the growth of *Arabidopsis thaliana* under high-light stress by reducing the accumulation of reactive oxygen species and maintaining photosynthesis. Under high-light stress, SA187 triggers dynamic changes in the expression of *Arabidopsis* genes related to fortified iron metabolism and redox regulation, thereby enhancing the antioxidative glutathione/glutaredoxin redox system of the plant. Genetic analysis showed that the enhancement of iron and sulfur metabolism by SA187 is coordinated by ethylene signaling. In summary, beneficial microbes could be an effective and inexpensive means of enhancing high-light-stress tolerance in plants.

Key words: high-light stress, beneficial plant–microbe interaction, redox regulation, glutaredoxins, ethylene signaling

Shekhawat K., Veluchamy A., Fatima A., García-Ramírez G.X., Reichheld J.-P., Artyukh O., Fröhlich K., Polussa A., Parween S., Nagarajan A.P., Rayapuram N., and Hirt H. (2024). Microbe-induced coordination of plant iron–sulfur metabolism enhances high-light-stress tolerance of *Arabidopsis*. Plant Comm. **5**, 101012.

INTRODUCTION

Light is a crucial factor for plants, serving as the primary energy source for photosynthesis and playing a significant role in plant growth and development. However, excessive light can be detrimental to plant growth by suppressing photosynthetic capacity, leading to oxidative damage of cellular organelles. There have been instances of excess daylight resulting in high-light (HL) stress for plants (d'Alessandro et al., 2020). For instance, in the Northern Hemisphere region (i.e., Wisconsin, USA), light intensity can be up to 1400 μmol m^{-2} s^{-1} and is assumed to be constant throughout the year (Handara et al., 2016). Under such HL conditions, excess electrons cannot be passed to photosystem I, and this results in the accumulation of multiple reactive oxygen species (ROS), including hydrogen peroxide (H_2O_2) and superoxide ($O_2^{\bullet -}$) (Apel and Hirt, 2004). In such circumstances, rapid plant response mechanisms like non-photochemical energy quenching dissipate the excess energy as heat (Goss and Lepetit, 2015; Ruban, 2016; Schumann et al., 2017; Shi et al., 2022). Non-photochemical energy quenching is a major factor in the rapid protection of photosystem II reaction centers from photodamage that would otherwise lead to photoinhibition of photosynthesis. Plants can also avoid damage from HL through changes in the composition of the photosynthetic apparatus, avoidance

Published by the Plant Communications Shanghai Editorial Office in association with Cell Press, an imprint of Elsevier Inc., on behalf of CSPB and CEMPS, CAS.

Please cite this article in press as: Shekhawat et al., Microbe-induced coordination of plant iron–sulfur metabolism enhances high-light-stress tolerance of *Arabidopsis*, Plant Communications (2024), https://doi.org/10.1016/j.xplc.2024.101012

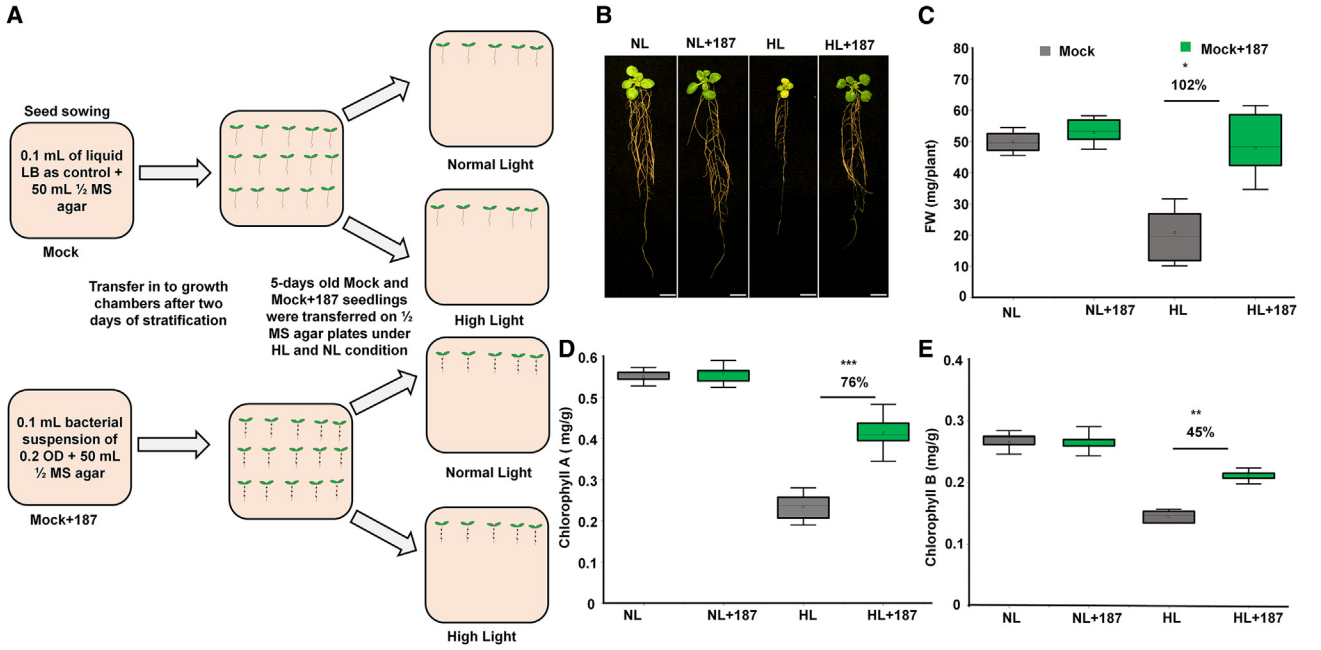

Figure 1. SA187 induces tolerance to high-light stress in *A. thaliana* and maintains chlorophyll A and B levels.

(A) Experimental setup: *A. thaliana* seedlings were germinated for 5 days with or without SA187. At day 6, colonized and non-colonized seedlings were transferred to fresh 1/2 MS, and the plates were exposed to a normal light (NL) intensity of 130 μmol m^{-2} s^{-1} or a high light (HL) intensity of 1050 μmol m^{-2} s^{-1} and grown vertically for 10 days.

(B) Phenotypic assessment of the beneficial effect of SA187 on the growth of 16-day-old *A. thaliana* seedlings under NL (NL and NL + 187) and HL (HL and HL + 187) conditions.

(C) Fresh weight of 16-day-old plants with and without SA187 under NL and HL regimes.

(D and E) Contents of chlorophyll A and chlorophyll B in SA187-colonized and non-colonized plants under NL control and HL-stress conditions. All plots represent the means of three biological replicates. Error bars indicate SD. Asterisks indicate a statistically significant difference based on Student's *t*-test: $^{*}P \leq 0.05$, $^{**}P \leq 0.01$, and $^{***}P \leq 0.001$ for comparisons between HL and HL+187 treatments. Scale bars correspond to 1 cm.

movements of chloroplasts and leaves, and changes in leaf morphology (Kasahara et al., 2002; Kim et al., 2005; Walters, 2005; Wada, 2013; Schöttler and Tóth, 2014). To survive and continue development under excess light, plants activate the transcription of genes encoding enzymes responsible for ROS scavenging (Rossel et al., 2002; Kleine et al., 2007; Jung et al., 2013). To compensate for ROS stress, plants also enhance glutathione (GSH) production to manage oxidative stress. GSH, the most abundant low-molecular-weight thiol in cells, is a redox buffer that keeps the intracellular environment in a reduced state (García-Quirós et al., 2020). GSH and glutaredoxins (GRXs) participate in the regeneration of enzymes involved in peroxide and methionine sulfoxide reduction, constituting an important cellular system for maintenance of redox homeostasis (Grant, 2001). It has recently been shown that GRXs can be engineered to confer enhanced oxidative stress tolerance to plants under abiotic stresses such as temperature and light stress (Cheng et al., 2011; Knuesting et al., 2015; Rey et al., 2017; Martins et al., 2020; Dard et al., 2023; Hendrix et al., 2023).

Although plants try to combat excess light conditions, they are not always successful in doing so, resulting in irreversible cellular damage or cell death. In this context, studies have demonstrated the effectiveness of plant-growth-promoting bacteria in promoting plant growth under abiotic stresses such as heat and iron (Fe) deficiency (Harbort et al., 2020; Shekhawat et al., 2022). In this work, we show that the beneficial endophytic bacterium *Enterobacter* sp. SA187 isolated from root nodules of *Indigofera argentea* can enhance the HL stress tolerance of *Arabidopsis thaliana* through coordination of Fe and sulfur (S) acquisition, thereby strengthening the plant antioxidative system. We also show that the beneficial effect of SA187 on HL stress is dependent on reprogramming of the plant transcriptome via the plant ethylene signaling pathway to enhance HL stress tolerance. Overall, we propose that microbes that live in association with plants could be an effective system for enhancing HL stress tolerance in crops.

RESULTS

SA187 induces HL stress tolerance in *A. thaliana*

To assess the effect of SA187 on the growth of *A. thaliana* under HL stress, we colonized *A. thaliana* plants with SA187 and exposed 5-day-old colonized and non-colonized plants to normal light (NL) at 130 μmol m^{-2} s^{-1} and HL at 1050 μmol m^{-2} s^{-1} (Figure 1A). Compared with NL exposure, exposure of non-colonized plants to HL led to chlorotic leaf damage (Figure 1B) and a 129% reduction in plant fresh weight (FW) (Figure 1C). By contrast, SA187-colonized *A. thaliana* plants were protected against chlorotic leaf damage under HL and continued to grow (Figure 1B). To investigate SA187-induced HL stress tolerance, we compared the FWs of SA187-colonized HL-treated plants (HL + 187) to those of non-colonized HL-treated plants (HL).

Please cite this article in press as: Shekhawat et al., Microbe-induced coordination of plant iron–sulfur metabolism enhances high-light-stress tolerance of *Arabidopsis*, Plant Communications (2024), https://doi.org/10.1016/j.xplc.2024.101012

HL + 187 plants exhibited 102% higher FWs than non-colonized plants (HL). This effect was specific to HL stress, as SA187-colonized plants (NL + 187) and non-colonized plants (NL) displayed similar growth (Figure 1B) and FW (Figure 1C) under NL control conditions. These data show that SA187 protects *A. thaliana* from HL stress and enhances plant growth.

SA187 improves plant growth under HL stress by increasing chlorophyll A and B levels

HL stress affects the photosynthetic machinery of plants and, consequently, chlorophyll content. To examine the performance of SA187-colonized plants under HL, we measured chlorophyll A and B contents. As shown in Figure 1D and 1E, compared with NL, HL stress significantly reduced chlorophyll A and B levels by 134% and 82%, respectively. However, compared with non-colonized HL plants, SA187-colonized HL plants showed significantly higher chlorophyll A and B levels (Figure 1D and 1E, 76% and 45%, respectively). SA187 colonization did not influence chlorophyll A and B levels under control NL conditions, indicating that SA187 mediates a beneficial effect on *A. thaliana* only under HL stress (Figure 1D and 1E).

Dynamic transcriptome responses of *A. thaliana* seedlings to different durations of HL stress

To investigate the molecular events underlying HL stress in *A. thaliana*, we performed transcriptome analysis of plants exposed to HL for 1 h, 24 h, or 5 days, together with their respective controls exposed to NL (Supplemental Figure 1A–1E). We performed pairwise comparisons (e.g., 1 h of NL versus 1 h of HL) to identify differentially expressed genes (DEGs) at each time point. The expression profiles of all DEGs upon HL stress fell into short-term (1 h), mid-term (24 h), and long-term (5 days) plant responses (Figure 2). Considering DEGs with $P \leq 0.05$ and fold change ≥ 2 or ≤ -2, a total of 1841 DEGs were observed at 1 h, 2324 DEGs at 24 h, and 2395 DEGs at 5 days of HL stress (Supplemental Datasheet 1).

To analyze transcriptional dynamics across different time points under HL stress, we first organized the transcriptome data into 20 clusters before performing gene ontology (GO) enrichment analysis (Figure 2). The transcriptome analysis of *A. thaliana* under HL stress revealed nuanced temporal responses, with distinct molecular events occurring during various phases of stress exposure. In the short term (1 h), we identified a set of 524 genes (cluster 2) that were exclusively upregulated. These genes were enriched in response to abiotic stimuli, cell redox homeostasis, and various stressors like HL intensity, oxidative stress, and heat stress. This immediate response indicated the activation of stress-related pathways to cope with the initial impact of HL. At 1 h and 24 h, we observed an upregulated cluster of 244 induced genes (cluster 4) that showed enrichment in responses to karrikin, water deprivation, abscisic acid, light stimulus, and acidic chemicals. Interestingly, a cluster of 564 genes (cluster 5) was gradually upregulated across all three time points (1 h, 24 h, and 5 days). Enriched terms for cluster 5 included autophagy, response to hypoxia, oxygen-containing compounds, and programmed cell death, suggesting a sustained and coordinated cellular response consistent with the observed HL-induced plant growth arrest over time. The 24-h HL response was notable for a cluster of 658 upregulated genes (cluster 10) enriched in categories such as S metabolism, anthocyanin and secondary metabolite biosynthesis, and redox processes. This behavior points to an active adaptive plant response to counteract the stress conditions and maintain cellular homeostasis. Clusters 18 and 19 contained genes specifically upregulated after 5 days of exposure, which were mainly involved in autophagy, hypoxia, and cell death.

We performed an additional analysis focusing on the 32 genes that were consistently upregulated in response to HL stress at all three timepoints (Supplemental Figure 2). These genes, including *ELIP1, HSP23.5, ROF2, HSP17.6A, HSP70b, HSP90.1, HOP3, and TIN1,* were enriched in HL intensity responses and can be regarded as HL signature genes. By contrast, 52 genes were consistently downregulated across all HL timepoints. Notably, this set included genes encoding components of the photosynthetic machinery, such as *PSBT* and *PSBF* (Supplemental Datasheet 2). These findings provide insight into the plant's sophisticated adaption dynamics and contribute to a broader understanding of plant stress responses.

SA187 dynamically reprograms *A. thaliana* transcription under HL

We next compared the molecular responses of non-colonized and SA187-colonized *A. thaliana* plants after 24 h and 5 days of exposure to HL stress. Compared with non-colonized plants and considering a fold change ≥ 1.6 or ≤ -1.6 ($P \leq 0.05$), 454 genes were differentially expressed in SA187-colonized plants after 24 h under NL conditions (Supplemental Datasheet 3). By contrast, 471 DEGs were found in SA187-colonized plants (HL + 187) compared with non-colonized plants (HL) after 24 h under HL stress (Supplemental Datasheet 3). Compared with non-colonized plants (HL), SA187-colonized plants (HL + 187) exhibited 414 DEGs after 5 days of HL. By contrast, compared with non-colonized plants (NL), SA187-colonized plants (NL + 187) exhibited only 82 DEGs after 5 days of NL (Supplemental Datasheet 3).

Under both NL and HL conditions, SA187 induced the expression of 18 genes at 24 hours. These genes were characteristic of typical bacterial response genes and included *PR1*, *PR5*, *SARD1*, and *FRK1*. After 5 days of HL exposure, 15 genes were induced (Supplemental Figure 3A and 3B), including *CYP71A12*, *CML46*, and *WRKY46* (Supplemental Datasheet 4). Notably, only three genes (*AED1*, *AT5G42530*, and *AT2G25510*) were consistently upregulated across all treatments (NL, NL + 187, HL, and HL + 187), and no common downregulated genes were identified in these treatments (Supplemental Figure 3C and 3D).

SA187 reprograms the *A. thaliana* transcriptome related to photosynthesis and oxidative stress in HL-stressed plants

We used heatmaps to better understand how SA187-colonized *A. thaliana* responded to HL conditions. The maps revealed differential gene expression patterns at 24 h in both NL and HL settings (Figure 3A). The DEGs identified at this 24-h time point were systematically categorized into 10 clusters. Cluster 1, comprising 45 genes, emerged as uniquely upregulated owing to SA187 colonization under NL. These genes were notably enriched in processes associated with lipid localization, transport, and macromolecule localization. Clusters 2 and 3, which contained 83 and 80 genes,

Please cite this article in press as: Shekhawat et al., Microbe-induced coordination of plant iron–sulfur metabolism enhances high-light-stress tolerance of *Arabidopsis*, Plant Communications (2024), https://doi.org/10.1016/j.xplc.2024.101012

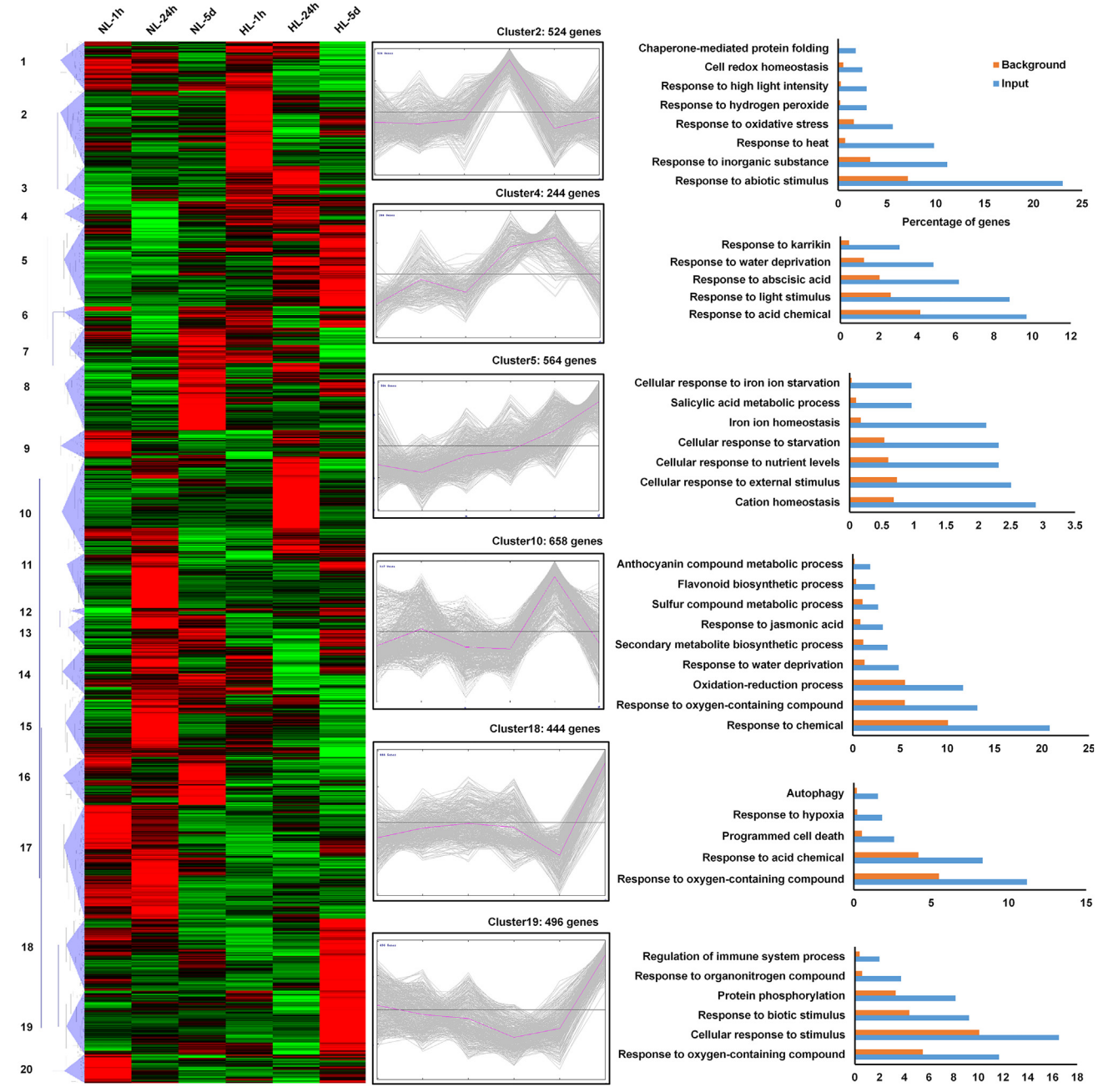

Figure 2. Dynamic transcriptome responses of *A. thaliana* seedlings to short-, middle-, and long-term high-light stress.
Hierarchical clustering of up- and downregulated DEGs in *A. thaliana* in response to 1 h, 24 h, and 5 days of normal light (NL) or high light (HL) exposure. For each gene, values of fragments per kilobase of transcript per million mapped reads were normalized. Red bars denote an increase in expression for a given gene, whereas green bars indicate a decrease. For the most relevant clusters, significantly enriched gene families are indicated on the basis of gene ontology. The pink line in each cluster indicates the overall trend of differentially expressed genes in that cluster for different treatments. Five-day-old seedlings were transferred to new 1/2 MS plates before NL and HL treatments. RNA-seq was performed with 1-h, 24-h, and 5-day HL-exposed plants and their respective NL controls. RNA-seq experiments were performed in three biological replicates.

respectively, exhibited a distinctive downregulation in non-colonized plants under HL, a phenomenon observed to a lesser extent in colonized plants under HL (HL + 187) (Figure 3A). Genes in cluster 2 were found to be responsive to metal-ion exposure and related to photosynthesis (including multiple *LHCBs*, *PSAs*, and *PSBs*), oxidative stress, and Fe binding (*cICDH*, *FER1*, *FER3*, *FER4*, and *MYB15*). By contrast, cluster 3 was characterized by enrichment in processes such as phosphorylation, response to hormone stimulus, amino acid metabolism, and phosphate metabolism. Cluster 5, which contained 159 genes, was specifically upregulated in colonized plants under HL conditions (HL + 187) (Figure 3A). These genes were notably enriched in responses to bacteria, salicylic acid stimulus, and redox metabolism and included key components such as

Please cite this article in press as: Shekhawat et al., Microbe-induced coordination of plant iron–sulfur metabolism enhances high-light-stress tolerance of *Arabidopsis*, Plant Communications (2024), https://doi.org/10.1016/j.xplc.2024.101012

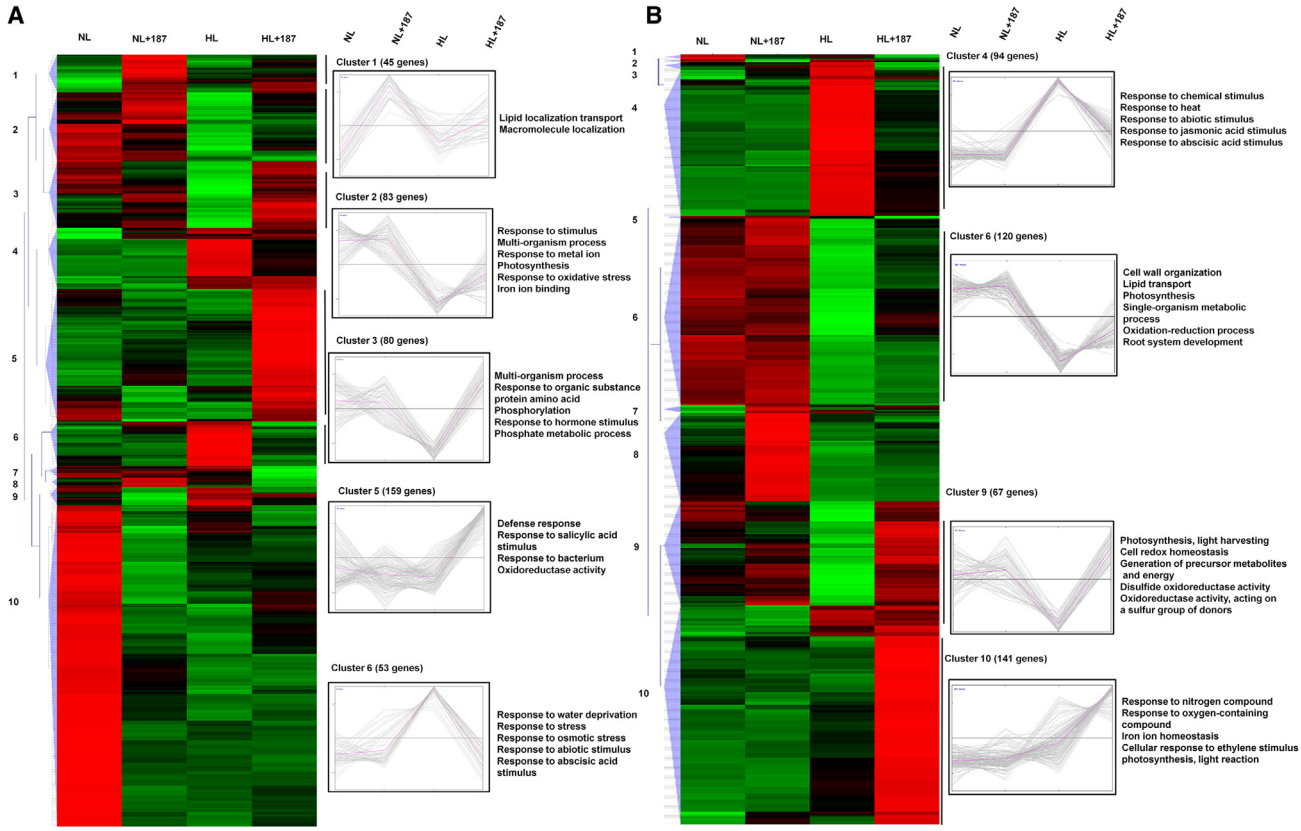

Figure 3. SA187 reprograms the *A. thaliana* transcriptome to improve photosynthesis and oxidative stress after 24 h and 5 days of HL stress.

(A) Hierarchical clustering of up- and downregulated DEGs in SA187-colonized and non-colonized *A. thaliana* seedlings in response to 24 h of normal light (NL) or high light (HL) exposure.

(B) Hierarchical clustering of up- and downregulated DEGs in SA187-colonized and non-colonized *A. thaliana* seedlings in response to 5 days of HL or NL exposure. Red bars denote an increase in expression for a given gene, and green bars indicate a decrease. For the most relevant clusters, significantly enriched gene families are indicated on the basis of gene ontology. Five-day-old seedlings ± SA187 were transferred to new 1/2 MS plates before NL and HL treatments. RNA-seq was performed with 24-h and 5-day HL-exposed plants and their respective NL controls with and without SA187. RNA-seq experiments were performed in three biological replicates.

peroxidases (*PRX*s), *ATBBE4/6/7*, *F6H1*, *ARD1*, *FRO2*, *GA2OX8*, *HO3*, *PAD3*, and *SAG13*. Finally, cluster 6 (53 genes) was exclusively induced in non-colonized plants under HL, whereas no corresponding induction was observed in colonized HL plants (HL + 187) (Figure 3A). These genes were enriched for responses to water deprivation, osmotic stress, and abscisic acid.

In summary, the 24-h transcriptome revealed distinct gene expression profiles related to photosynthesis (Supplemental Figure 3E) and oxidative stress management in SA187-colonized *A. thaliana*, highlighting a refined regulatory response compared with that of non-colonized plants under HL conditions.

Transcriptome data reveal that SA187 modulates plant redox status via GRXs under long-term HL stress

We used a transcriptome heatmap to examine *A. thaliana* responses to prolonged HL stress (Figure 3B). Four gene clusters revealed distinct expression patterns (Figure 3B). Cluster 4 consisted of 94 genes that showed higher transcript levels in non-colonized plants under HL treatment but not in colonized plants (HL + 187) (Figure 3B). These genes were enriched in response to heat and response to jasmonic acid and abscisic acid. Cluster 6 contained 120 genes that were downregulated in non-colonized plants under HL and showed less downregulation in SA187-colonized plants (HL + 187) (Figure 3B). These genes were enriched in cell-wall organization, lipid transport, photosynthesis, redox metabolism, and root development. Similarly, cluster 9 included 67 genes that were downregulated in non-colonized plants (HL) but upregulated by SA187 (HL + 187) under HL conditions (Figure 3B). These genes were enriched in GO terms related to photosynthesis, light harvesting (*CAB2*, *LHCB2.1*, *PSBE*, *PSBH*, and *PSBI*), redox homeostasis (*ROXY6*, *8*, *9*, *12*, *14*, and *20*), generation of precursor metabolites and energy, and disulfide and S-group redox metabolism. Cluster 10, likewise, was enriched primarily in HL + 187 and to a lesser extent in HL plants, and showed specific enrichment of terms such as response to nitrogen compounds, oxygen-containing compounds, Fe-ion homeostasis, ethylene, and photosynthesis. The presence of SA187 increased the transcript levels of 22 genes involved in the photosynthetic process. These included *PSAD-2*, *LHCB6*, *CAB2*, *PSAH2*, *LHCB2.1*, *LHCB2.2*, *PSBX*, *LHCB4.3*, *PSAH-1*, *PSBTN*, *PSBQ-2*, *RBCS2B*, *RBCS1B*, *LHCB3*, *PSAN*, *PSBK*, *PSBI*, *PSBZ*, *PSBJ*, *PSBH*, *PSAC*, and

Please cite this article in press as: Shekhawat et al., Microbe-induced coordination of plant iron–sulfur metabolism enhances high-light-stress tolerance of *Arabidopsis*, Plant Communications (2024), https://doi.org/10.1016/j.xplc.2024.101012

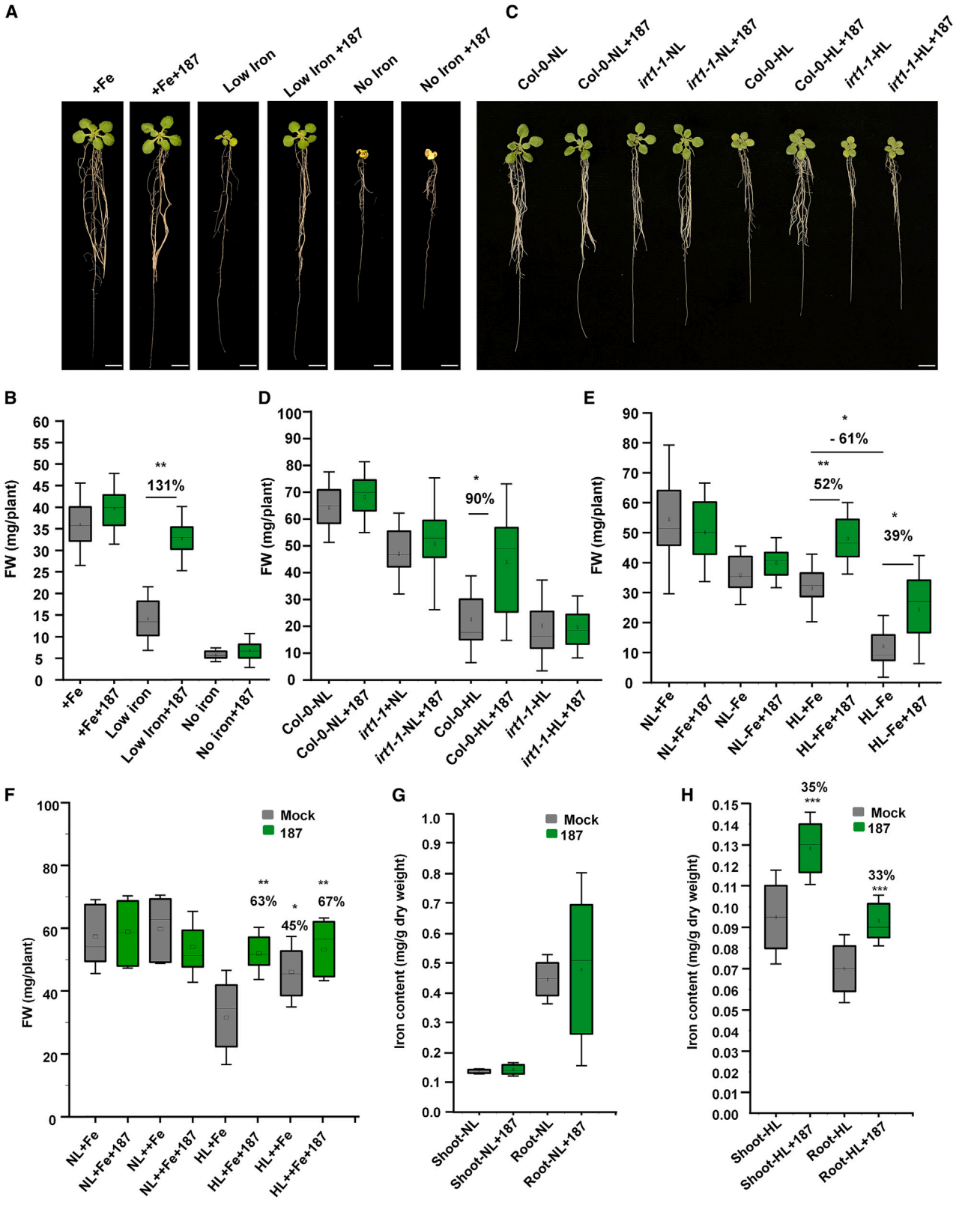

Figure 4. SA187-mediated plant growth rescue under high-light stress involves iron.

(A) Phenotypic assessment of the effect of SA187 inoculation on growth of *A. thaliana* seedlings under +Fe (sufficient iron, 18 mg/l FeNaEDTA), low-iron (4 mg/l FeNaEDTA), and no-iron (0 mg/l FeNaEDTA) conditions.

(B) Fresh weight of 16-day-old plants with and without SA187 grown under +Fe (sufficient iron), low-iron, and no-iron conditions.

(legend continued on next page)

Please cite this article in press as: Shekhawat et al., Microbe-induced coordination of plant iron–sulfur metabolism enhances high-light-stress tolerance of *Arabidopsis*, Plant Communications (2024), https://doi.org/10.1016/j.xplc.2024.101012

NDHE (Supplemental Figure 3E). Transcriptome data from NL + 187 and HL + 187 plants at 5 days indicated that SA187 colonization maintained the expression of genes associated with photosynthesis and redox balance orchestrated by GRXs and the biogenesis of Fe–S cluster proteins (Supplemental Figure 4). The regulation of these genes suggests that SA187 positively influences the expression of key genes related to light harvesting, photosystem components, and electron transport, ultimately contributing to enhanced plant photosynthetic activity.

SA187 reprograms the plant proteome under long-term HL stress

After 5 days of HL exposure, we performed liquid chromatography–tandem mass spectrometry protein analysis of SA187-colonized *A. thaliana*. Using a threshold of fold change $\geq$ 1.6 and $P \leq 0.05$, 40 proteins increased, and 34 decreased (Supplemental Datasheet 5). Upregulated proteins showed enrichment in the GO terms cytoplasm, organelle envelope, plastid, and chloroplast. Interestingly, despite no overlap with the transcriptome, both analyses highlighted enrichment in photosynthesis-related GO categories. Overall, without considering *P* values, we identified 965 differentially expressed proteins, with 408 upregulated and 275 downregulated in SA187-colonized HL plants (Supplemental Datasheet 5). GO analysis of the 408 upregulated proteins revealed GO terms such as response to ROS, glycosyl compound and tetrapyrrole metabolism, chloroplast, plastid thylakoid, and Fe–S cluster binding (Supplemental Datasheet 5). Although only six proteins showed an overlap between the upregulated transcriptome and proteome, similar GO categories, such as photosynthesis, response to ROS, and Fe–S cluster binding, were obtained. Among the six common genes in the overlap between proteome and transcriptome, two photosystem II proteins (PSBH and PsbTn) showed enhanced abundance in colonized plants (Supplemental Figure 5). The enriched Fe–S cluster binding category included the following six proteins: Fe–S center of cytochrome *b6f* complex PETC, Fe–S cluster protein ARABIDOPSIS MITOCHONDRIAL FERREDOXIN 1, FERREDOXIN C 2, CHLOROPHYLL A OXYGENASE, 2Fe–2S ferredoxin-like superfamily protein, and methylthiotransferase (Supplemental Datasheet 3). These results support the hypothesis that SA-187-colonized plants can grow under HL conditions because of enhanced resilience of the photosystems via continued biosynthesis of Fe–S proteins.

The role of Fe in SA187-mediated rescue of plant growth under HL stress

Fe is crucial for plant function, especially during photosynthesis. Analysis of transcriptome data at 24 h and 5 days of HL stress (Supplemental Figure 6) revealed enrichment of Fe-related genes in colonized plants. These genes encompassed various aspects of Fe metabolism, including the Fe starvation response (e.g., *AT5G40510*, *NPF2.5*, *ATAGP22*, *RHS13*, and *ZIP3*), Fe uptake and transport (e.g., *FRO2*, *FRO4*, *FRO6*, *IRT2*, and *F6H1*), and Fe storage (e.g., *FER1*, *FER3*, and *FER4*). We therefore asked whether SA187 could help to promote Fe uptake by *A. thaliana* under low-Fe conditions. As seen in Figure 4A and 4B, *A. thaliana* showed a 171% reduction in FW under low-Fe conditions (low Fe; 4 mg FeNaEDTA/l) but demonstrated a 131% growth improvement with SA187 colonization (low Fe + 187). Control experiments with no Fe (0 mg/l) revealed no growth of SA187-colonized or non-colonized plants, indicating that SA187 requires at least a minimal quantity of Fe for growth rescue (Figure 4A and 4B). To further characterize the role of Fe in SA187-induced HL tolerance, we used the *irt1-1* mutant, which is deficient in Fe uptake. *irt1-1* plants showed a growth deficit and leaf chlorosis phenotype under HL stress. In contrast to that of wild-type plants, the phenotype of *irt1-1* mutant plants was not improved by colonization with SA187 (Figure 4C and 4D), indicating an important role for Fe import in the mechanism of SA187-induced tolerance to HL stress. To eliminate possible discrepancies in bacterial colonization, we evaluated the effects of the *irt1-1* mutation and HL stress on SA187 colonization. At 5 and 10 days of HL stress, there were no significant differences in colony-forming units (CFUs) between Col-0 and *irt1-1* mutants, indicating that the mutation does not affect the overall colonization of *A. thaliana* under NL or HL conditions (Supplemental Figure 7). Under low-Fe conditions (8 mg/l), plants exposed to HL stress (HL −Fe) exhibited a 61% reduction in FW compared with Fe-sufficient conditions (HL +Fe) (Figure 4E). Conversely, under low-Fe conditions, SA187-colonized plants (HL −Fe + 187) outperformed non-colonized plants (HL −Fe) (Figure 4E). Higher FeNaEDTA levels in the medium under HL stress (HL ++Fe) produced significant growth benefits, akin to SA187 colonization (Figure 4F). The addition of Fe increased FW by 80% (HL ++Fe) compared with non-treated HL plants (HL +Fe). Notably, the combination of SA187 and increased FeNaEDTA (HL +Fe + 187) produced the greatest FW increase (110%) under HL stress (Figure 4F). Fe levels in the shoot and root were assessed in non-colonized and SA187-colonized plants under NL and HL conditions (Figure 4G and 4H). Under NL conditions, SA187 inoculation did not affect Fe concentrations. However, under HL conditions, SA187 increased Fe levels in the shoot and root by 35% and 33%, respectively (Figure 4H).

S plays an important role in SA187-mediated HL-stress tolerance

S is essential for photosynthesis because of its roles in protein synthesis, enzyme activity, chlorophyll production, and redox

(C and D) Phenotypic assessment **(C)** and fresh-weight analysis **(D)** of SA187-colonized and non-colonized Col-0 and *irt1-1* mutant plants (deficient in iron import) grown under NL and HL conditions for 10 days.

(E) Fresh weight of 16-day-old SA187-colonized and non-colonized *A. thaliana* seedlings grown on +Fe (sufficient iron, 18 mg/l FeNaEDTA) or −Fe (low iron, 8 mg/l FeNaEDTA) 1/2 MS medium plates under NL and HL regimes.

(F) Fresh weight of Col-0 plants after doubling the Fe concentration (++Fe; 36 mg/l FeNaEDTA) under NL and HL regimes with and without SA187.

(G) Shoot and root iron content of SA187-colonized and non-colonized plants under NL.

(H) Shoot and root iron content of SA187-colonized and non-colonized plants under HL stress measured by ICP–OES (inductively coupled plasma optical emission spectroscopy). All plots represent the means of three biological replicates. Error bars indicate SD. Asterisks indicate a statistically significant difference based on Student's *t*-test: $^{*}P \leq 0.05$, $^{**}P \leq 0.01$, and $^{***}P \leq 0.001$ for comparisons of HL with HL + 187 treatments and HL ++Fe (36 mg/l FeNaEDTA).

Please cite this article in press as: Shekhawat et al., Microbe-induced coordination of plant iron–sulfur metabolism enhances high-light-stress tolerance of *Arabidopsis*, Plant Communications (2024), https://doi.org/10.1016/j.xplc.2024.101012

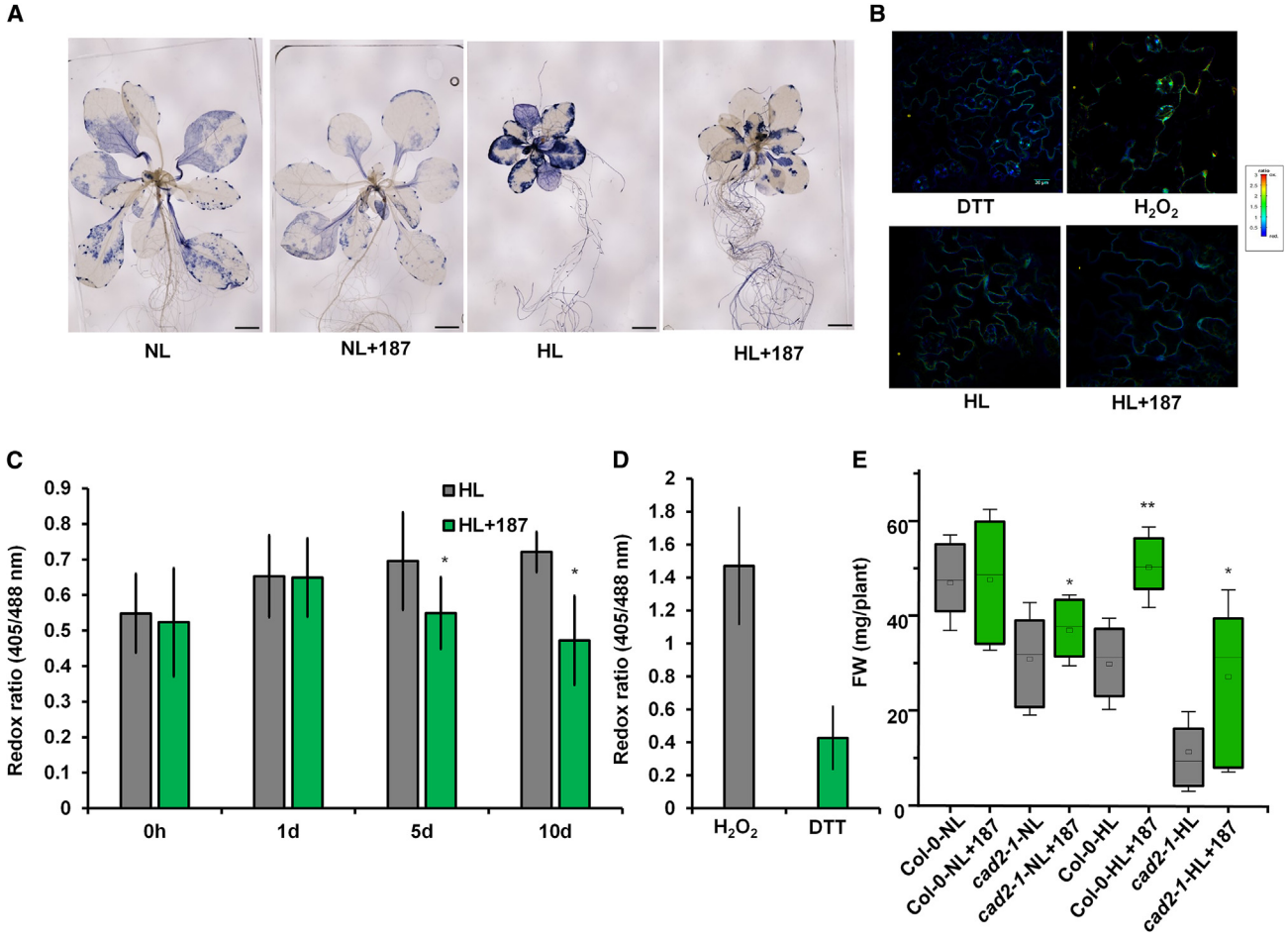

Figure 5. SA187 reduces ROS levels to maintain plant photosynthetic performance under high-light stress.

(A) Accumulation of superoxide radicals (visualized by nitroblue tetrazolium staining) in NL (normal light, control) and HL (high-light stress) ± SA187 plants.

(B) *In vivo* monitoring of redox state upon high-light stress. Cytosolic ro-GFP2 fluorescence from confocal images of plants treated with DTT or H_2O_2 (top two images) and SA187 colonized and non-colonized plant leaves after 5 days of high-light stress. Cytosolic ro-GFP2 fluorescence signals were collected at 505–530 nm after excitation with either 405 nm or 488 nm.

(C) Redox ratios were calculated as the 405/488 nm fluorescence from SA187-colonized and non-colonized plants exposed to HL stress for 0 h, 24 h, 5 days, and 10 days.

(D) Redox ratios were calculated as the 405/488 nm fluorescence from 10 mM DTT-treated and 100 mM H_2O_2-treated 10-day-old plants.

(E) Fresh weight of SA187-colonized or non-colonized wild-type Col-0 and *cad2-1* mutant plants upon long-term exposure to NL and HL treatments. All plots represent the means of three biological replicates. Error bars indicate SE. Asterisks indicate a statistically significant difference based on Student's *t*-test: $^{*}P \leq 0.05$, $^{**}P \leq 0.01$, and $^{***}P \leq 0.001$ for comparisons between HL and HL + 187 treatments. Scale bars correspond to 1 cm.

regulation. HL stress can damage Fe–S proteins, mainly in photosystem I and ferredoxin. Our transcriptome data revealed DEG enrichment of S compound and amino acid metabolic processes after 24 h and 5 days of HL exposure in colonized plants, including *BGLU34*, *BGLU35*, *BCAT6*, *CYP81F2*, *IGMT1*, *NAC042*, and *WRKY70* (Supplemental Figure 8). In addition, genes encoding Fe–S cluster proteins (*ABCI*, *NEET*, and *PSAC*) were upregulated under HL + 187 conditions. Increased sulfate concentrations in the medium have also been reported to help plants to withstand various abiotic stresses such as salt stress. We therefore compared the growth of plants under HL stress with increased $MgSO_4$ levels in the medium (Supplemental Figure 9). Under HL stress, the addition of sulfate (HL + S) had significant beneficial effects on plant growth, similar to colonization by SA187 (Supplemental Figure 9). The addition of sulfate increased FW by 90% (HL + S) compared with that of non-treated HL plants (mock + HL). Examining *sultr1;2*, *sir1-1*, and *IsuC* mutant plants highlighted the key role of plant S metabolism in HL-stress tolerance. Importantly, SA187 showed the ability to enhance the growth of these mutants under HL stress, highlighting its potential as a stress ameliorator (Supplemental Figure 9).

SA187 reduces ROS levels and affects cytoplasmic redox state under HL stress

HL stress induces ROS production in the chloroplast, and one of the major drastic effects of ROS is the inhibition of the photosynthetic machinery. To test the possibility that SA187 protects *A. thaliana* from excessive ROS levels, we examined superoxide levels in SA187-colonized and non-colonized plants grown under NL and HL-stress conditions. Nitroblue tetrazolium staining showed that SA187 colonization did not enhance superoxide

Please cite this article in press as: Shekhawat et al., Microbe-induced coordination of plant iron–sulfur metabolism enhances high-light-stress tolerance of *Arabidopsis*, Plant Communications (2024), https://doi.org/10.1016/j.xplc.2024.101012

radical levels under NL conditions (Figure 5A). However, under HL conditions, SA187-colonized plants (HL + 187) showed reduced superoxide levels compared with non-colonized HL plants (Figure 5A). Because HL-induced ROS can disturb the redox status of cells, we compared the redox status of SA187-colonized to non-colonized plants under HL stress. We used a cytosolic GRX1/ro-GFP2-tagged reporter line to monitor the response of *A. thaliana* to HL-imposed redox changes in SA187-colonized and non-colonized plantlets. The ro-GFP2 fluorescence signals were collected at 505–530 nm after excitation at either 405 nm or 488 nm. The ratio of images was calculated as 405/488 nm fluorescence. When evaluating the ro-GFP2 redox ratio, focusing specifically on the leaf cytosol (Figure 5C), we noted gradual partial oxidation after 24 h, 5 days, and 10 days of HL. By contrast, there was a progressive reduction in SA187-colonized plants under HL (HL + 187). The redox ratios were significantly higher in non-colonized plants compared with SA187-colonized plants at 5 and 10 days of HL stress (Figure 5B and 5C). After 10 days of HL, non-colonized plants showed a 405/488 ratio of 0.72 (partial oxidation), whereas SA187-colonized plants showed a ratio of 0.45 (fully reduced), indicating that SA187-colonized plants have a fortified redox balance under HL stress. As controls, we used 10 mM DTT and 100 mM H_2O_2 to fully reduce or oxidize ro-GFP2 (Figure 5B and 5D). ro-GFP2 monitors GSH redox homeostasis. Because GSH synthesis is tightly linked to ROS protection, one possible explanation for these results could be that SA187-colonized plants have a higher redox capacity due to improved GSH synthesis. To assess this possibility, we used *cad2-1* mutants, which are characterized by a deficiency in γ-glutamylcysteine synthetase, a pivotal enzyme in GSH biosynthesis. *cad2-1* mutant plants exhibited slowed growth phenotypes under normal conditions due to reduced GSH synthesis. However, the growth of *cad2-1* mutants was ameliorated in the presence of SA187. When subjected to HL stress, non-colonized plants exhibited significant growth inhibition, in contrast to SA187-colonized plants (Figure 5E). These findings emphasize the role of SA187 in maintaining GSH levels, providing a protective effect against damage induced by HL stress.

SA187 improves plant thiol redox balance under HL conditions

The generation of ROS induced by HL leads to protein inactivation through oxidation of thiol groups. To assess this, we measured the thiol content of SA187-colonized and non-colonized plants under NL and HL-stress conditions at days 5 and 10. At day 5, HL treatment resulted in a nine-fold reduction in total protein thiol (PT) compared with NL conditions (Supplemental Figure 10A). However, SA187-colonized plants exhibited a slight increase in PT content under both NL and HL conditions (Supplemental Figure 10A). Moreover, plants colonized by SA187 exhibited increased non-protein thiol (NPT) content under HL stress, potentially attributable to elevated GSH (Supplemental Figure 10B), contributing to an overall increase in total cellular thiol compared with non-colonized plants (Supplemental Figure 10C). Notably, these findings provide additional support for the SA187-mediated growth rescue of *cad2-1* mutant plants. After 10 days of HL stress, SA187-colonized plants demonstrated a reduction in NPT content and a 92% increase in PT content compared with non-colonized HL plants (Supplemental Figure 11). These findings suggest that the presence of SA187 alleviates PT oxidation in HL-treated plants but also induces NPT levels in the context of HL.

Plant GRXs play an important role in SA187-mediated HL-stress tolerance

GRXs are key proteins that protect cells from oxidative stress and are known to be involved in the biogenesis of Fe–S clusters, as well as redox reactions (Lill and Muhlenhoff, 2008; Rouhier et al., 2008, 2010). Because our transcriptome data showed enrichment for transcripts of different GRXs and disulfide oxidoreductase activity, we examined the role of the cytosolic Fe–S cluster GRX GRXS17 in SA187-mediated HL-stress tolerance. Colonized and non-colonized *grxs17* mutant plants were subjected to NL and HL conditions. As shown in Supplemental Figure 10D, the *grxs17* mutant plants suffered significantly more under HL stress than the wild-type plants, exhibiting a 70% reduction in FW (Supplemental Figure 10D and 10E). Unlike wild-type *Arabidopsis*, which were protected from HL stress (112% higher FW compared with non-colonized HL-treated plants), SA187-colonized *grxs17* mutant plants showed less beneficial effect of SA187 under HL stress (Supplemental Figure 10D and 10E). These results indicate the importance of GRXs in the mechanism of SA187-mediated HL-stress tolerance in plants.

Ethylene is a key regulator of SA187-mediated HL-stress tolerance

The transcriptome analysis of plants at 5 days of HL treatment revealed significant GO-term enrichment for ethylene in SA187-colonized plants compared with their non-colonized counterparts. This enrichment encompassed various aspects of ethylene biosynthesis and signaling and involved genes such as *ACS4*, *ACS6*, *ACS5*, *ETO2*, *ERF2*, *ERF13*, *ERF15*, *TN7*, *AT1G28370*, *AT4G29780*, *ATAVT6B*, and *WRKY40* (Figure 3B) (Supplemental Figure 8). Moreover, previous studies have shown that ethylene is a key regulator of SA187-mediated plant growth under heat and salt stress (de Zélicourt et al., 2018; Shekhawat et al., 2021). To test whether ethylene also plays a role in SA187-induced HL-stress tolerance, we analyzed the ethylene-insensitive *ein3-1* mutant under NL and HL conditions. Unlike the wild type, *ein3-1* mutants were compromised in SA187-mediated HL-stress resistance, indicating that EIN3 is involved in SA187-mediated HL-stress tolerance (Figure 6A). We further confirmed these results in ethylene-insensitive *ein2-1* mutant plants (Supplemental Figure 12A and 12B). Fe uptake is regulated by ethylene (Lucena et al., 2015), and we therefore also analyzed whether SA187 effects were compromised in ethylene mutants under low-Fe conditions. Unlike in wild-type plants, SA187 could not restore the phenotype of *ein3-1* mutants under low-Fe conditions (Figure 6B). These results indicate that the ethylene pathway is also involved in SA187-mediated enhanced Fe uptake under conditions of normal light intensity. To confirm that ethylene signaling mediates the HL-stress tolerance conferred by SA187, we performed RT–qPCR of *FRO2 and LHCB genes in ein3-1* mutant plants after 24 h and 5 days of HL treatment. SA187-colonized *ein3-1* plants were compromised in the induction of higher transcript levels of these genes under HL stress compared with wild-type plants, confirming the EIN3-dependent induction of

Please cite this article in press as: Shekhawat et al., Microbe-induced coordination of plant iron–sulfur metabolism enhances high-light-stress tolerance of *Arabidopsis*, Plant Communications (2024), https://doi.org/10.1016/j.xplc.2024.101012

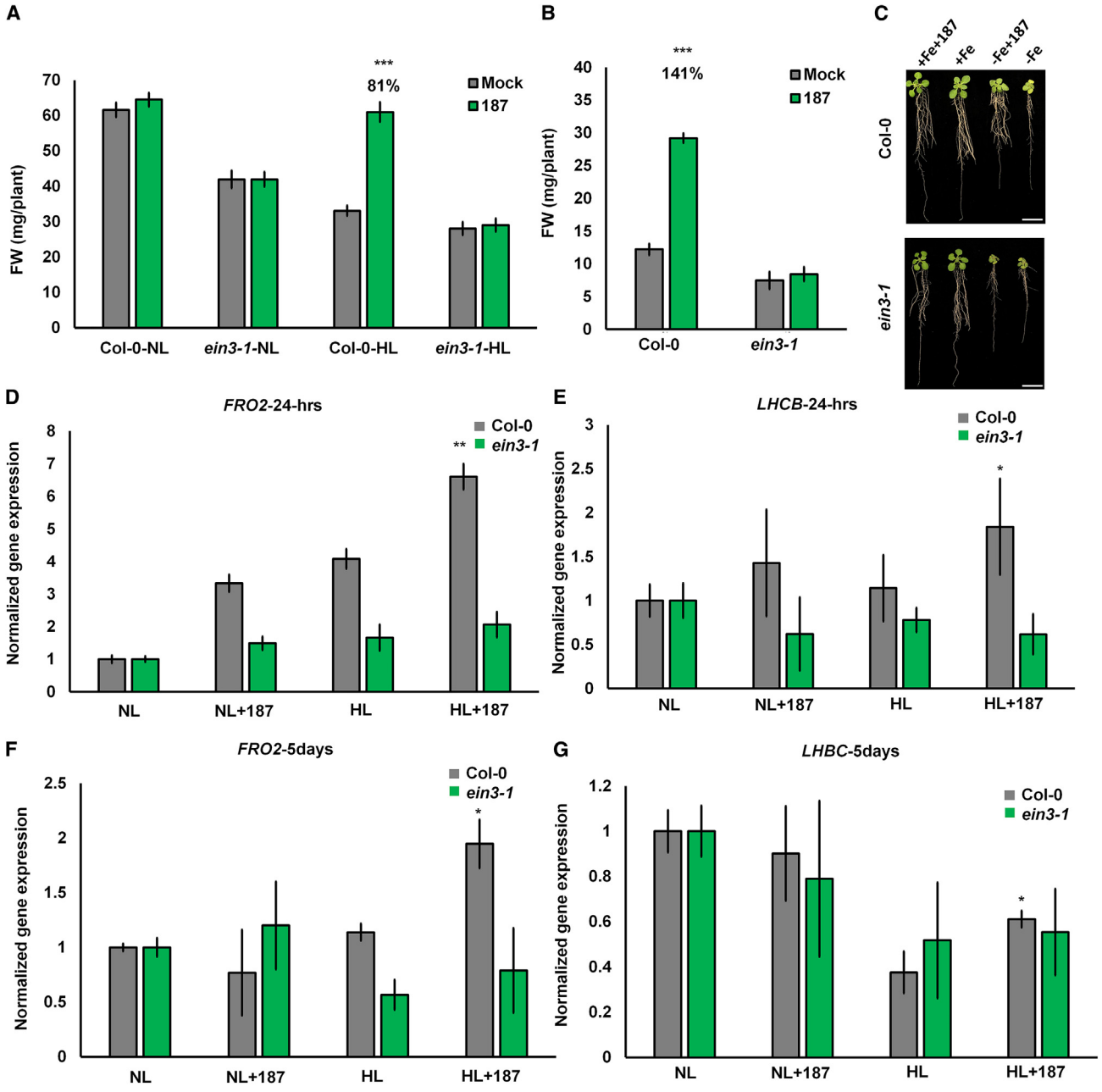

Figure 6. Ethylene is a main regulator of SA187-mediated high-light-stress tolerance.

(A) Fresh weight of SA187-colonized or non-colonized wild-type Col-0 and *ein3-1* mutant plants upon long-term exposure to normal light (NL) and high light (HL).

(B and C) Fresh weight and phenotypic assessment of SA187-colonized and non-colonized wild-type Col-0 and *ein3-1* mutant plants under low-iron conditions (4 mg/l FeNaEDTA).

(D and E) Transcript levels of *FRO2* (ferric reduction oxidase 2) and *LHCB* (light-harvesting chlorophyll A/B-binding protein) in Col-0 and *ein3-1* mutant plants after 24 h of NL (NL and NL + 187) or HL exposure (HL and HL + 187).

(F and G) Transcript levels of *FRO2* (ferric reduction oxidase 2) and *LHCB* (light-harvesting chlorophyll A/B-binding protein) in Col-0 and *ein3-1* mutant plants after 5 days of NL (NL and NL + 187) or HL exposure (HL and HL + 187). For analysis of transcript levels, the data were normalized to tubulin as a reference gene. All plots represent the means of three biological replicates. Error bars indicate SE. Asterisks indicate a statistically significant difference based on Student's *t*-test: $^{*}P \leq 0.05$, $^{**}P \leq 0.01$, and $^{***}P \leq 0.001$ for comparisons between HL and HL + 187 treatments. Scale bars correspond to 1 cm.

HL-stress tolerance conferred by SA187 (Figure 6C and 6F). We further confirmed this hypothesis by verifying the expression of *IGMT1*, *BCAT6*, *LSU1*, *CYP17A12*, *HO3*, and *FER4* (Supplemental Figure 13). To eliminate possible discrepancies in bacterial colonization, we evaluated the effect of the *ein2-1* mutation and HL stress on SA187 colonization. At 5 and 10 days of HL stress, Col-0 and *ein2-1* mutants showed no significant differences in CFU levels, indicating that the ethylene mutant did not differ in overall SA187 colonization under NL or HL conditions (Supplemental Figure 7).

Please cite this article in press as: Shekhawat et al., Microbe-induced coordination of plant iron–sulfur metabolism enhances high-light-stress tolerance of *Arabidopsis*, Plant Communications (2024), https://doi.org/10.1016/j.xplc.2024.101012

DISCUSSION

Light is vital for plant growth, serving as the main energy source. However, excess light absorption can lead to increased production of ROS, causing photo-oxidative damage and inhibiting photosynthesis. Our data confirm previous reports that plants respond to short-, mid-, and long-term HL stress through dynamic transcriptional changes (Huang et al., 2019). Transcriptome analysis revealed the relative dynamics of transcriptional changes. Complex transcriptional responses occur in plants when exposed to different timescales of HL stress. The novelty of our work is that microbes can assist plants in maintaining growth under such stress conditions (Figure 1B and 1C). Mitochondria and chloroplasts rely on abundant Fe and S for essential functions such as photosynthesis, respiration, DNA repair, and ribosome biogenesis, all of which are facilitated by Fe–S-cluster-containing proteins (Rouhier et al., 2010). Our research reveals the mechanisms by which SA187-mediated ethylene signaling orchestrates Fe and S metabolism, bolstering *Arabidopsis* tolerance to HL stress. Under HL, plants accumulate ROS, which impair the Fe–S cluster proteins that are vital for photosynthesis. Transcriptomic and phenotypic analyses revealed that SA187 enhances plant uptake of Fe and S, supporting the synthesis of Fe–S cluster proteins essential for maintenance of the photosynthetic machinery under stress. Moreover, we found that SA187 colonization rescued plant growth under Fe-limiting conditions during HL stress. Supplementation with Fe and S similarly enhanced plant resilience to HL, akin to SA187 colonization. SA187 promotes Fe acquisition by upregulating root-associated (*FRO2*, *FRO4*, *FRO6*, and *IRT2*) and chloroplast-associated (*FER1*, *FER3*, *FER4*, *ZIP3*, and *HO3*) Fe genes. The increased transcripts of root-associated genes could be attributed to the enhanced root formation observed in plants colonized by SA187 under HL-stress conditions. Whereas previous studies have highlighted the beneficial role of microbes in aiding plants under Fe-limiting conditions (Zamioudis et al., 2014; Verbon et al., 2017; Harbort et al., 2020; Montejano-Ramírez and Valencia-Cantero, 2023), our study brings forth a novel aspect by revealing that microbes can also confer protection to plants under HL stress, which induces Fe limitation. This finding highlights the complex role of microbial colonization in plant resilience, particularly under challenging environmental conditions such as HL stress. Proteomic analysis verified increased levels of Fe–S cluster and photosystem proteins in SA187-colonized plants after 5 days of HL exposure. In addition, $MgSO_4$ supplementation improved plant performance under HL stress. Analysis of *sultr1;2*, *sir1-1*, and *lsuC* mutant plants underscores the pivotal role of plant S metabolism in HL-stress tolerance. Remarkably, SA187 enhances the growth of these mutants under HL stress, highlighting its potential as a stress ameliorator. Photosynthetic organisms have evolved a variety of direct and indirect mechanisms for HL-stress management, including ROS production/scavenging, stomatal regulation, and systemic signaling (Mignolet-Spruyt et al., 2016; Huang et al., 2019; Barczak-Brzyżek et al., 2022; Shi et al., 2022). In this context, our data reveal that SA187 induces the expression of several peroxidases, such as *PRX31*, *37*, *69*, and *71*, at 24 h, whereas *PRX01* and *2*, *FSD1*, and other peroxidases accumulate under long-term HL. Higher expression of these peroxidases helps plants to scavenge ROS and maintain photosynthetic activity (Fryer et al., 2003; Lu et al., 2017; Melicher et al., 2022). In addition, the antioxidative process relies on GSH, which facilitates the reduction of disulfide-containing proteins by GRXs (Gleason and Holmgren, 1988; Holmgren, 1989). GRXs undergo oxidation by substrates and are non-enzymatically reduced by GSH. This GSH/GRX system plays a crucial role in maintaining redox homeostasis (Grant, 2001). Multiple pieces of evidence suggest that GSH and GRXs play a role in responding to oxidative stress by regenerating the enzymes involved in disulfide protein reduction. Moreover, GRXs are versatile proteins involved in various functions, including Fe–S cluster biogenesis, encompassing Fe and S acquisition, cluster assembly, transfer, and maintenance. Our data from HL-stress experiments on both colonized and non-colonized plants demonstrate that the presence of SA187 boosts the expression of a cluster of at least eight GRX genes after 5 days of exposure to HL. This implies that SA187 prompts elevation of the GRX/GSH system to reinforce redox equilibrium. This hypothesis is supported by loss of the beneficial effect of SA187 in *grxs17* mutant plants under HL stress. GRXs can be engineered to enhance oxidative stress tolerance in plants and for investigation of redox-controlled processes in temperature-stress tolerance (Kapoor et al., 2015; Martins et al., 2020; Kumar et al., 2021). AtGRXS17 plays a role in oxidative stress response, tolerance to Fe deficiency, and thermotolerance in both yeast and plants (Wu et al., 2012; Yu et al., 2017; Cheng et al., 2020), and transgenic expression of *PvGrx5 from the* fern *Pteris vittata* in *A. thaliana* increases tolerance to high-temperature stress and reduces oxidative damage to proteins (Sundaram and Rathinasabapathi, 2010). Proper performance of the GRX/GSH system is involved in maintaining the thiol redox balance of thiol proteins. We therefore also examined the PT and NPT content of SA187-colonized and non-colonized plants under NL and HL conditions. PT contents decreased under HL treatment, particularly in SA187-colonized plants. Moreover, the NPT content was higher in SA187-colonized plants than in non-colonized plants under HL. These data show that SA187 maintains PT status by improving the antioxidant system. Oxidative stress is expected to increase S flux to S reduction for production of the redox buffer GSH/GSSG. We suggest that SA187 helps to improve both S and Fe homeostasis to maintain redox balance and thereby reduce HL-induced oxidative damage in *A. thaliana* (Figure 7).

We found that ethylene was crucial for SA187-induced HL-stress tolerance in plants. Our findings highlighted the compromised HL tolerance of *ein3-1* mutant plants, underlining the importance of the ethylene pathway and the EIN3 transcription factor. Moreover, ethylene signaling is vital for regulation of Fe uptake mechanisms, as shown by the poor growth of *ein3-1* mutants under Fe-limited conditions. Interestingly, SA187-colonized *ein3-1* plants showed compromised growth under low-Fe conditions, unlike their wild-type counterparts. This observation suggests that SA187-induced ethylene signaling is vital for maintaining an adequate Fe supply during HL stress. Previous research has also shown that EIN3 upregulates FIT1 under Fe-deficiency conditions, thus influencing the expression of *IRT1* and *FRO2* genes (Yang et al., 2022). Modification of phytohormone synthesis in plants by beneficial microbes influences plant responses to Fe deficiency. Similarly, ethylene signaling in *A. thaliana* plays a role in regulating the S regulon, which encompasses a significant portion of S metabolic enzymes.

Please cite this article in press as: Shekhawat et al., Microbe-induced coordination of plant iron–sulfur metabolism enhances high-light-stress tolerance of *Arabidopsis*, Plant Communications (2024), https://doi.org/10.1016/j.xplc.2024.101012

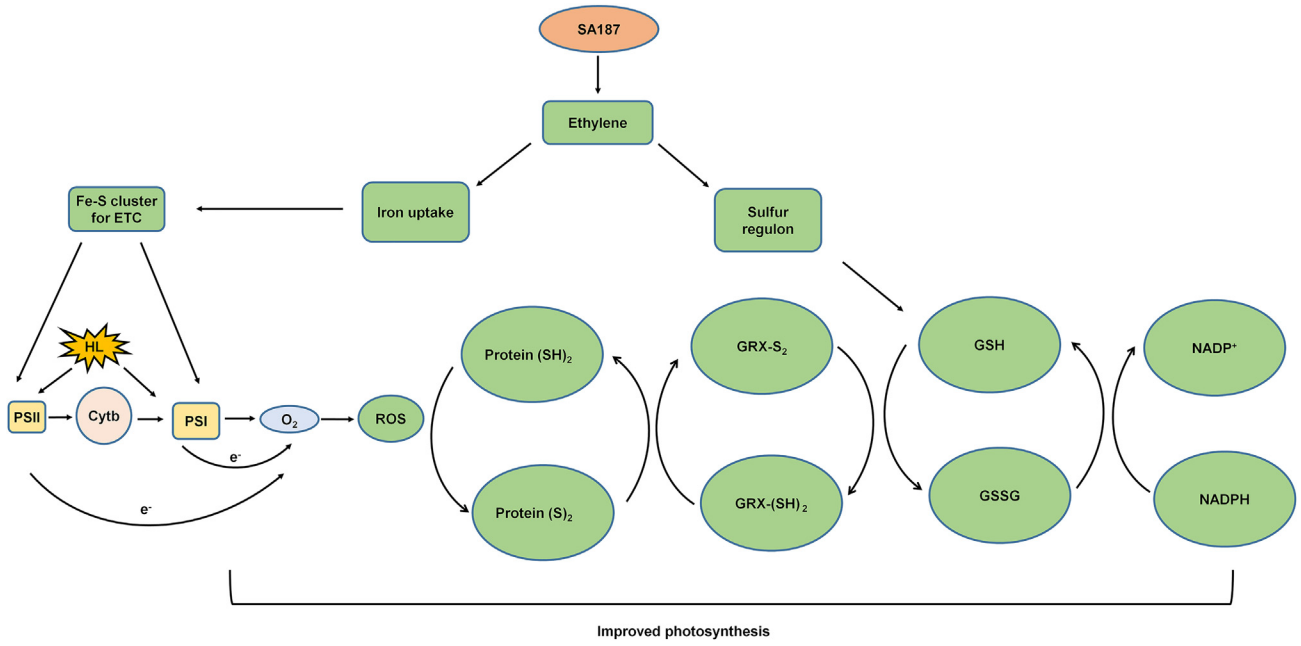

Figure 7. A model representing SA187-mediated high-light-stress tolerance in *A. thaliana* through ethylene-dependent iron-assisted redox metabolism.

The model illustrates ethylene-dependent SA187-induced iron (Fe) and sulfur (S) metabolism in *Arabidopsis*. SA187-induced Fe metabolism plays a crucial role in the biogenesis of Fe–S clusters and the maintenance of Fe–S cluster-containing proteins, which are essential for the electron transport chain (ETC). In addition, SA187-induced sulfate is used for the formation of Fe–S clusters and can be converted into glutathione (GSH). GSH, in turn, participates in reducing the oxidation of thiol-containing proteins through GSH/glutaredoxin-dependent redox metabolism, ultimately mitigating high-light-induced ROS. HL, high-light; PSII, photosystem II; Cytb, cytochrome *b*; PSI, photosystem I; O_2, oxygen; ROS, reactive oxygen species; protein (SH), thiol-containing protein; protein $(S)_2$, disulfide protein; $GRX(S)_2$, oxidized glutaredoxins; $GRX(SH)_2$, reduced glutaredoxins; GSH, reduced glutathione; GSSG, oxidized glutathione; $NADP^+$, oxidized nicotinamide adenine dinucleotide phosphate; NADPH, reduced nicotinamide adenine dinucleotide phosphate.

This regulation influences sulfate uptake, contributing to the synthesis of precursors for protein synthesis and antioxidants like GSH for mitigation of cellular ROS levels. The reduced upregulation of Fe and S genes observed in SA187-colonized *ein3-1* plants (Figure 7; Supplemental Figure 13) highlights the central role of ethylene in orchestrating plant responses to Fe and S homeostasis under stress conditions, helping to explain why SA187-induced ethylene signaling is crucial for sustaining Fe and S levels during HL stress. We also analyzed the SA187 genome, revealing the presence of genes encoding enterobactin and aerobactin siderophores (Supplemental Figure 14A). Results on Chrome Azurol S (CAS) plates also demonstrated siderophore production by SA187 (Supplemental Figure 14B). Genes involved in Fe metabolism (*entB*, *YbdZ*, Enterobactin synthase components B and F, ferric aerobactin receptor, and *FepD*) (Supplemental Figure 15) were upregulated after 6 h of growth on CAS plates compared with LB medium, as well as in colonized plants under HL stress compared with NL conditions (specifically *entB* and *YbdZ*) (Supplemental Figure 15B–15D). These findings support the idea that SA187 makes use of its Fe metabolism to enhance plant growth under HL-stress conditions.

In summary, our data support the notion that colonization with SA187 can shield plants from extreme oxidative stress conditions such as HL stress. These findings highlight the nuanced effect of microbial colonization on plant stress resilience, particularly in sustaining crucial processes like photosynthesis and redox homeostasis. Protection against these stresses is achieved through ethylene-dependent signaling that enhances Fe and S acquisition, ultimately fortifying the antioxidative redox system. As a result, SA187 helps to maintain photosynthesis and overall plant growth under challenging HL-stress conditions.

METHODS

Bacterial inoculum and medium preparation

The endophytic bacterial strain *Enterobacter* sp. SA187 was isolated from root nodules of *I. argentea* collected from the Jizan region of Saudi Arabia (Andrés-Barrao et al., 2017). Before the plant colonization experiments were performed, the cryogenically maintained SA187 strain was streaked out on LB agar medium and incubated at 28°C for 24 h. A single colony was used for further experiments. For bacterial seed plates, 50 ml of half-strength Murashige and Skoog medium (1/2 MS) with 0.9% agar and a pH of 5.8 was mixed with 0.1 ml of fresh bacterial suspension with an OD of 0.2 to obtain a final concentration of 10^5 CFU ml^{-1}. For control plates, 0.1 ml of liquid LB was mixed with 1/2 MS medium.

Plant material and growth conditions for *A. thaliana*

A. thaliana wild-type Col-0 seeds and mutants (*irt1-1*, *ein3-1*, *cad2-1*, and *sir1-1*) were obtained from publicly available collections, and seeds of GRX1/ro-GFP2 and *grxs17* mutant lines were obtained from Jean-Philippe Reichheld's laboratory. Seeds were surface sterilized with 0.05% SDS, then washed three times with

Please cite this article in press as: Shekhawat et al., Microbe-induced coordination of plant iron–sulfur metabolism enhances high-light-stress tolerance of *Arabidopsis*, Plant Communications (2024), https://doi.org/10.1016/j.xplc.2024.101012

absolute ethanol. The sterilized seeds were plated on 1/2 MS medium agar plates seeded with 10^5 CFU ml^{-1} SA187. Seeds were stratified at 4°C for 2 days, and the plates were then transferred to growth chambers (Model CU36-L5, Percival Scientific, Perry, IA, USA) for growth. For HL experiments, after 5 days, SA187-inoculated and non-inoculated seedlings of near equal lengths were transferred to new 1/2 MS plates. For the HL-stress experiment, SA187 treated and non-treated control plants were transferred to a 16-h HL intensity of 1050 μmol m^{-2} s^{-1} in a Biochamber (Huang et al., 2019). For control conditions, the colonized and non-colonized plants were transferred to a 16-h NL intensity of 130 μmol m^{-2} s^{-1}. Light levels were measured with an SPR-03 spectroradiometer (Luzchem). The temperature of the HL chamber was maintained by cool airflow from the bottom of the chamber to ensure that the medium and leaf temperatures were kept at 22°C to match the control growth conditions. Samples were harvested after 1 h, 24 h, and 5 days of HL treatment. The control plants were kept in the 130 μmol m^{-2} s^{-1}, 22°C chamber, and control samples were collected at each time point. Sterile conditions were maintained throughout the experiment by ensuring that the plates were securely sealed with surgical tape, effectively preventing any external contamination from compromising the results.

Chlorophyll measurements

Chlorophylls A and B were extracted from frozen shoot samples (50 mg) with 80% acetone (Arnon, 1949; Sims and Gamon, 2002). After centrifugation, the supernatant was used to measure OD at 537, 647, 645, and 663 nm. The following formulas were used to calculate chlorophyll A/B: chlorophyll A (μmol ml^{-1}) = 0.01373 A663 − 0.000897 A537 − 0.003046 A647; chlorophyll B (μmol ml^{-1}) = 0.02405 A647 − 0.004305 A537 − 0.005507 A663.

RNA extraction, reverse transcription, and RT–qPCR

For RNA-sequencing (RNA-seq) analysis, total plant RNA was extracted from colonized and non-colonized plants exposed to NL and HL-stress conditions using the NucleoSpin RNA Plant kit (Macherey-Nagel), including DNase I treatment, according to the manufacturer's recommendations. For qPCR analysis, total RNA was reverse transcribed using Superscript III (Invitrogen): 1 μg of total RNA and oligo(dT) as primer were used for cDNA synthesis according to the manufacturer's protocol. For *A. thaliana* gene expression analyses, tubulin was used as the reference gene. All reactions were performed in a CFX96 Touch Real-Time PCR Detection System (Bio-Rad) as follows: 50°C for 2 min, 95°C for 10 min, and 40 cycles of 95°C for 10 s and 60°C for 40 s. All reactions were performed with three biological replicates, and each reaction was performed in technical triplicate. The reference gene used in this analysis was ACTIN2 (At3g18780), and gene expression was normalized against the reference gene.

Bioinformatics analysis of RNA-seq data

The concentration and purity of RNA were determined by spectrophotometry, and RNA integrity was confirmed using an Agilent 2100 Bioanalyzer with an RNA 6000 Nano Assay kit (Agilent Technologies, Palo Alto, CA, USA). RNA samples with an RNA integrity number greater than 8 and a 280:260 ratio greater than 2 were used for RNA-seq. We constructed mRNA libraries from total plant RNA using the Illumina mRNA Library Prep kit and sequenced them on the Illumina HiSeq 4000 platform. We checked the quality of the sequenced reads using FASTQC (Andrews, 2010). Low-quality reads or base pairs, as well as adaptors, were trimmed using Trimmomatic v.0.36 (Bolger et al., 2014). The trimmed reads were aligned to the combined TAIR10 and SA187 genomes using TopHat v.2.2.1 (Trapnell et al., 2009, 2012; Kim et al., 2013). Reads per million bases and differential expression between two conditions were calculated using Cufflinks v.2.2.0 (Trapnell et al., 2009). To identify DEGs, specific parameters ($P \leq 0.05$; Benjamini–Hochberg statistical correction; false discovery rate [FDR] ≤ 0.05) in cuffdiff were used. Post-processing and visualization of differential expression were performed using cummeRbund v.2.0.0. A cutoff of 2-fold change and P value less than 0.05 was used to identify up- and downregulated genes between NL and HL conditions, whereas a cutoff of 1.6-fold change and $P \leq 0.05$ was used to identify up- and downregulated genes between the HL and HL + 187 treatments. AgriGO (Tian et al., 2017) was used to find the corresponding GO terms (FDR ≤ 0.05) and functions of the respective genes. Venny (Oliveros, 2007) was used to identify common or unique genes. The clustering analysis was performed using MeV (MultiExperiment Viewer) software, which enabled us to organize and interpret the complex datasets, providing insights into the relationships and patterns within the gene expression data.

Quantification of SA187 colonization

Seedlings were initially cultivated on 1/2 MS agar plates inoculated with SA187, and 5-day-old seedlings were subsequently transferred to fresh 1/2 MS plates. On the sixth day, the plants were subjected to NL and HL exposure for 5 days and 10 days to perform CFU analysis. The plants were homogenized by grinding. Each resulting sample was suspended in 1 ml of extraction buffer containing 10 mM $MgCl_2$ and 0.01% Silwet L-77. Serial dilutions were performed, and the diluted samples were plated onto LB agar plates. After incubation overnight at 28°C, CFUs were counted. The calculated CFU values were normalized to the weight of the plant material (per milligram).

Protein extraction and sample preparation

A. thaliana wild-type plants were grown under HL and NL conditions for 5 days. The plants were harvested, frozen, and powdered. Proteins were extracted using a lysis buffer and then purified through a series of steps, including methanol/chloroform precipitation. The resulting proteins were quantified and digested into peptides. After desalting, the samples were prepared for mass spectrometry analysis using data-independent acquisition (DIA) to study the plant's protein content. This workflow allowed for a detailed analysis of protein changes in response to different light conditions.

DIA–MS analysis

The peptide samples (1.5 μg) were subjected to DIA–MS analysis using an Orbitrap Fusion Lumos mass spectrometer (Thermo Scientific) coupled with an UltiMate 3000 UHPLC (Thermo Scientific), following the methodology outlined in Zhang et al. (2019). The peptides were desalted, separated over a 130-min gradient, and analyzed in triplicate injections. DIA-MS data

were collected for three precursor mass ranges (400–650 *m/z,* 650–900 *m/z,* and 900–1200 *m/z*) with isolation windows of 6–8 Da. High-energy collisional dissociation (HCD) collision energy was set to 30%, and MS parameters included resolutions of 60 000 for MS1 and 30 000 for MS/MS. The protocol used EASY-IC for internal mass calibration, and the maximum ion accumulation time was 100 ms with a target value of 1e6.

DIA–MS data analysis

DIA–MS data were analyzed using Spectronaut software (version 14) with an *A. thaliana* spectral library generated in-house. Default Biognosys settings were used for identification, and a paired Student's *t*-test was performed to identify differentially expressed proteins between control and mutant samples. A multiple testing correction was applied to control the FDR. Proteins with a fold change greater than 1.5 were considered to be differentially expressed. GO enrichment analysis was performed using AgriGO (v.2) and Revigo to reduce redundant GO terms.

Quantification of total thiol, NPT, and PT contents

Total thiol (TT) and PT contents were determined according to Sedlak and Lindsay (1968). *A. thaliana* seedlings (50 mg) were homogenized in 1000 μl of 0.2 M Tris–HCl (pH 7.4) and centrifuged at 10 000 *g* for 20 min at 4°C. The supernatant was used to assay TT and NPT. To determine TT content, 50 μl of supernatant was mixed with 150 μl of 0.2 mM Tris–HCl (pH 8.2), 10 μl of 0.01 M DTNB (5,5-dithio-bis-(2-nitrobenzoic acid), and 790 μl of absolute methanol. The yellow color that developed was measured after 15 min at 415 nm against a blank vial containing 50 μl of distilled water instead of supernatant. Total sulfhydryl groups were calculated on the basis of an extinction coefficient of 13 600 and expressed as μmol/g FW. To determine NPT content, 500 μl of supernatant was mixed with 400 μl of distilled water and 100 μl of 50% TCA (Trichloroacetic acid). After 15 min, the mixture was centrifuged at 10 000 *g* for 15 min. Using 200 μl of deproteinized supernatant, NPT concentration was measured as described for TT. PT was calculated by subtracting NPT content from TT content.

Confocal microscopy of ro-GFP2

SA187-colonized and non-colonized HL-stress-treated GRX1/ro-GFP2 seedlings were imaged using an inverted Zeiss LSM 880 confocal microscope equipped with Plan-Apochromat 10×/0.45, Plan-Apochromat 20×/0.8, and Plan-Apochromat 40×/1.4 oil objectives and ZEN 2010 software (Zeiss). The excitation of ro-GFP2 in HL-treated colonized and non-colonized seedlings was performed at 488 nm and 405 nm, and a band-pass (BP 490–555 nm) emission filter was used to collect the ro-GFP2 signal. Image analysis and quantification of ro-GFP2 redox ratios (405/488) were performed using Redox Ratio Imaging software (Fricker, 2016).

CAS assay for siderophore detection

Siderophore production was determined using the blue agar CAS assay as described in Louden et al. (2011). SA187 was spotted onto CAS plates and incubated at 28°C for 48 h. The appearance of a clear zone around and beneath the spotted culture indicated a positive result for siderophore production.

DATA AND CODE AVAILABILITY

The data supporting the results of this article are included within the article and its additional files. The raw data from the RNA-seq samples are available at the NCBI Gene Expression Omnibus under accession no. GSE251796 (https://www.ncbi.nlm.nih.gov/geo/query/acc.cgi?acc=GSE251796). The raw mass spectrometry proteomics data have been deposited at the ProteomeXchange Consortium via the PRIDE partner repository with the dataset identifier PXD047231.

SUPPLEMENTAL INFORMATION

Supplemental information is available at *Plant Communications Online*.

FUNDING

This publication is based upon work supported by the King Abdullah University of Science and Technology (KAUST) base fund for H.H. no. BAS/1/1062-01-01. J.-P.R. was supported by the Agropolis Fondation (Flagship Project CalClim grant no. 1802-002).

AUTHOR CONTRIBUTIONS

K.S. and H.H. conceived and designed the study. K.S. standardized the high-light stress protocol and phenotyping experiments and analyzed the data. A.V. performed bioinformatics analysis on the raw RNA-seq data, and A.P. assisted in RNA-seq library preparation. N.R. carried out proteome data analysis. A.F., O.A., and G.X.G.-R. contributed to phenotyping experiments, and K.F. provided support with confocal microscopy. S.P. submitted the RNA-seq data and assisted with analysis. J.-P.R. supervised the ro-GFP2 experiments. A.P.N. analyzed the SA187 genome. H.H. supervised the experiments and data analysis. K.S. and H.H. wrote the manuscript. H.H., J.-P.R., and N.R. edited the manuscript. All authors approved the final version of the manuscript.

ACKNOWLEDGMENTS

We thank all the members of the Hirt Lab and the CDA management and greenhouse facility team of KAUST for technical assistance. No conflict of interest is declared.

Received: April 15, 2024
Revised: June 11, 2024
Accepted: June 27, 2024

REFERENCES

Andrés-Barrao, C., Lafi, F.F., Alam, I., de Zélicourt, A., Eida, A.A., Bokhari, A., Alzubaidy, H., Bajic, V.B., Hirt, H., and Saad, M.M. (2017). Complete genome sequence analysis of Enterobacter sp. SA187, a plant multi-stress tolerance promoting endophytic bacterium. Front. Microbiol. **8**:2023.

Andrews, S. (2010). FastQC: A Quality Control Tool for High Throughput Sequence Data: Babraham Bioinformatics (Cambridge, United Kingdom: Babraham Institute).

Apel, K., and Hirt, H. (2004). Reactive oxygen species: metabolism, oxidative stress, and signal transduction. Annu. Rev. Plant Biol. **55**:373–399.

Arnon, D. (1949). Copper Enzymes in Isolated Chloroplasts. Polyphenoloxidase in Beta Vulgaris. Plant Physiol. **24**:1–15.

Barczak-Brzyżek, A., Brzyżek, G., Koter, M., Siedlecka, E., Gawroński, P., and Filipecki, M. (2022). Plastid retrograde regulation of miRNA expression in response to light stress. BMC Plant Biol. **22**:150.

Bolger, A.M., Lohse, M., and Usadel, B. (2014). Trimmomatic: a flexible trimmer for Illumina sequence data. Bioinformatics **30**:2114–2120.

Cheng, N.-H., Liu, J.-Z., Liu, X., Wu, Q., Thompson, S.M., Lin, J., Chang, J., Whitham, S.A., Park, S., Cohen, J.D., and Hirschi, K.D. (2011). Arabidopsis monothiol glutaredoxin, AtGRXS17, is critical for temperature-dependent postembryonic growth and development via modulating auxin response. J. Biol. Chem. **286**:20398–20406.

Cheng, N., Yu, H., Rao, X., Park, S., Connolly, E.L., Hirschi, K.D., and Nakata, P.A. (2020). Alteration of iron responsive gene expression in Arabidopsis glutaredoxin S17 loss of function plants with or without iron stress. Plant Signal. Behav. **15**:1758455.

d'Alessandro, S., Beaugelin, I., and Havaux, M. (2020). Tanned or sunburned: how excessive light triggers plant cell death. Mol. Plant **13**:1545–1555.

de Zélicourt, A., Synek, L., Saad, M.M., Alzubaidy, H., Jalal, R., Xie, Y., Andrés-Barrao, C., Rolli, E., Guerard, F., Mariappan, K.G., et al. (2018). Ethylene induced plant stress tolerance by Enterobacter sp. SA187 is mediated by 2-keto-4-methylthiobutyric acid production. PLoS Genet. **14**:e1007273.

Dard, A., Weiss, A., Bariat, L., Auverlot, J., Fontaine, V., Picault, N., Pontvianne, F., Riondet, C., and Reichheld, J.-P. (2023). Glutathione-mediated thermomorphogenesis and heat stress responses in Arabidopsis thaliana. J. Exp. Bot. **74**:2707–2725.

Fryer, M.J., Ball, L., Oxborough, K., Karpinski, S., Mullineaux, P.M., and Baker, N.R. (2003). Control of Ascorbate Peroxidase 2 expression by hydrogen peroxide and leaf water status during excess light stress reveals a functional organisation of Arabidopsis leaves. Plant J. **33**:691–705.

Fricker, M.D. (2016). Quantitative redox imaging software. Antioxid. Redox Signal. **24**:752–762.

García-Quirós, E., Alché, J.D., Karpinska, B., and Foyer, C.H. (2020). Glutathione redox state plays a key role in flower development and pollen vigour. J. Exp. Bot. **71**:730–741.

Gleason, F.K., and Holmgren, A. (1988). Thioredoxin and related proteins in procaryotes. FEMS Microbiol. Rev. **4**:271–297.

Goss, R., and Lepetit, B. (2015). Biodiversity of NPQ. J. Plant Physiol. **172**:13–32.

Grant, C.M. (2001). Role of the glutathione/glutaredoxin and thioredoxin systems in yeast growth and response to stress conditions. Mol. Microbiol. **39**:533–541.

Handara, V.A., Illya, G., Tippabhotla, S.K., Shivakumar, R., and Budiman, A.S. (2016). Center for Solar Photovoltaics (CPV) at Surya University: novel and innovative solar photovoltaics system designs for tropical and near-ocean regions (an overview and research directions). Procedia Eng. **139**:22–31.

Harbort, C.J., Hashimoto, M., Inoue, H., Niu, Y., Guan, R., Rombolà, A.D., Kopriva, S., Voges, M.J.E.E.E., Sattely, E.S., Garrido-Oter, R., et al. (2020). Root-Secreted Coumarins and the Microbiota Interact to Improve Iron Nutrition in Arabidopsis. Cell Host Microbe **28**:825–837.e6. https://doi.org/10.1016/j.chom.2020.09.006.

Hendrix, S., Dard, A., Meyer, A.J., and Reichheld, J.-P. (2023). Redox-mediated responses to high temperature in plants. J. Exp. Bot. **74**:2489–2507.

Holmgren, A. (1989). Thioredoxin and glutaredoxin systems. J. Biol. Chem. **264**:13963–13966.

Huang, J., Zhao, X., and Chory, J. (2019). The Arabidopsis transcriptome responds specifically and dynamically to high-light stress. Cell Rep. **29**:4186–4199.e3.

Jung, H.-S., Crisp, P.A., Estavillo, G.M., Cole, B., Hong, F., Mockler, T.C., Pogson, B.J., and Chory, J. (2013). Subset of heat-shock transcription factors required for the early response of Arabidopsis to excess light. Proc. Natl. Acad. Sci. USA **110**:14474–14479.

Kapoor, D., Sharma, R., Handa, N., Kaur, H., Rattan, A., Yadav, P., Gautam, V., Kaur, R., and Bhardwaj, R. (2015). Redox homeostasis in plants under abiotic stress: role of electron carriers, energy metabolism mediators and proteinaceous thiols. Front. Environ. Sci. **3**:13.

Kasahara, M., Kagawa, T., Oikawa, K., Suetsugu, N., Miyao, M., and Wada, M. (2002). Chloroplast avoidance movement reduces photodamage in plants. Nature **420**:829–832.

Kim, D., Pertea, G., Trapnell, C., Pimentel, H., Kelley, R., and Salzberg, S.L. (2013). TopHat2: accurate alignment of transcriptomes in the presence of insertions, deletions and gene fusions. Genome Biol. **14**:R36.

Kim, G.-T., Yano, S., Kozuka, T., and Tsukaya, H. (2005). Photomorphogenesis of leaves: shade-avoidance and differentiation of sun and shade leaves. Photochem. Photobiol. Sci. **4**:770–774.

Kleine, T., Kindgren, P., Benedict, C., Hendrickson, L., and Strand, A. (2007). Genome-wide gene expression analysis reveals a critical role for CRYPTOCHROME1 in the response of Arabidopsis to high irradiance. Plant Physiol. **144**:1391–1406.

Knuesting, J., Riondet, C., Maria, C., Kruse, I., Bécuwe, N., König, N., Berndt, C., Tourrette, S., Guilleminot-Montoya, J., Herrero, E., et al. (2015). Arabidopsis glutaredoxin S17 and its partner, the nuclear factor Y subunit C11/negative cofactor 2α, contribute to maintenance of the shoot apical meristem under long-day photoperiod. Plant Physiol. **167**:1643–1658.

Kumar, A., Kumar, V., Dubey, A.K., Ansari, M.A., Narayan, S., Meenakshi, K.S., Pandey, V., Pande, V., Sanyal, I., and Sanyal, I. (2021). Chickpea glutaredoxin (CaGrx) gene mitigates drought and salinity stress by modulating the physiological performance and antioxidant defense mechanisms. Physiol. Mol. Biol. Plants **27**:923–944.

Lill, R., and Muhlenhoff, U. (2008). Maturation of iron-sulfur proteins in eukaryotes: mechanisms, connected processes, and diseases. Annu Rev Biochem **77**:669–700.

Louden, B.C., Haarmann, D., and Lynne, A. (2011). Use of blue agar CAS assay for siderophore detection. J. Microbiol. Biol. Educ. **12**:51–53. https://doi.org/10.1128/jmbe.v12i1.249.

Lucena, C., Romera, F.J., García, M.J., Alcántara, E., and Pérez-Vicente, R. (2015). Ethylene participates in the regulation of Fe deficiency responses in Strategy I plants and in rice. Front. Plant Sci. **6**:1056.

Lu, T., Meng, Z., Zhang, G., Qi, M., Sun, Z., Liu, Y., and Li, T. (2017). Sub-high temperature and high-light intensity induced irreversible inhibition on photosynthesis system of tomato plant (Solanum lycopersicum L.). Front. Plant Sci. **8**:365.

Martins, L., Knuesting, J., Bariat, L., Dard, A., Freibert, S.A., Marchand, C.H., Young, D., Dung, N.H.T., Voth, W., Debures, A., et al. (2020). Redox modification of the iron-sulfur glutaredoxin GRXS17 activates holdase activity and protects plants from heat stress. Plant Physiol. **184**:676–692.

Melicher, P., Dvořák, P., Krasylenko, Y., Shapiguzov, A., Kangasjärvi, J., Šamaj, J., and Takáč, T. (2022). Arabidopsis iron superoxide dismutase FSD1 protects against methyl viologen-induced oxidative stress in a copper-dependent manner. Front. Plant Sci. **13**:823561.

Mignolet-Spruyt, L., Xu, E., Idänheimo, N., Hoeberichts, F.A., Mühlenbock, P., Brosché, M., Van Breusegem, F., and Kangasjärvi, J. (2016). Spreading the news: subcellular and organellar reactive oxygen species production and signalling. J. Exp. Bot. **67**:3831–3844.

Montejano-Ramírez, V., and Valencia-Cantero, E. (2023). Cross-Talk between Iron Deficiency Response and Defense Establishment in Plants. Int. J. Mol. Sci. **24**:6236. https://doi.org/10.3390/ijms24076236.

Oliveros, J.. Venny. An interactive tool for comparing lists with Venn Diagrams. http://bioinfogp.cnb.csic.es/tools/Venny/index.html.

Rey, P., Becuwe, N., Tourrette, S., and Rouhier, N. (2017). Involvement of Arabidopsis glutaredoxin S14 in the maintenance of chlorophyll content. Plant Cell Environ. **40**:2319–2332.

Rossel, J.B., Wilson, I.W., and Pogson, B.J. (2002). Global changes in gene expression in response to high-light in Arabidopsis. Plant Physiol. **130**:1109–1120.

Rouhier, N., Couturier, J., Johnson, M.K., and Jacquot, J.-P. (2010). Glutaredoxins: roles in iron homeostasis. Trends Biochem. Sci. **35**:43–52.

Rouhier, N., Lemaire, S.D., and Jacquot, J.P. (2008). The role of glutathione in photosynthetic organisms: Emerging functions for glutaredoxins and glutathionylation. Annu Rev Plant Biol **59**:143–166.

Ruban, A.V. (2016). Nonphotochemical chlorophyll fluorescence quenching: mechanism and effectiveness in protecting plants from photodamage. Plant Physiol. **170**:1903–1916.

Schöttler, M.A., and Tóth, S.Z. (2014). Photosynthetic complex stoichiometry dynamics in higher plants: environmental acclimation and photosynthetic flux control. Front. Plant Sci. **5**:188.

Schumann, T., Paul, S., Melzer, M., Dörmann, P., and Jahns, P. (2017). Plant growth under natural light conditions provides highly flexible short-term acclimation properties toward high-light stress. Front. Plant Sci. **8**:681.

Sedlak, J., and Lindsay, R.H. (1968). Estimation of total, protein-bound, and nonprotein sulfhydryl groups in tissue with Ellman's reagent. Anal. Biochem. **25**:192–205.

Shekhawat, K., Almeida-Trapp, M., Garcia-Ramirez, G.X., and Hirt, H. (2022). Beat the heat: plant- and microbe-mediated strategies for crop thermotolerance. Trends Plant Sci **27**:802–813.

Shekhawat, K., Saad, M.M., Sheikh, A., Mariappan, K., Al-Mahmoudi, H., Abdulhakim, F., Eida, A.A., Jalal, R., Masmoudi, K., and Hirt, H. (2021). Root endophyte induced plant thermotolerance by constitutive chromatin modification at heat stress memory gene loci. EMBO Rep. **22**:e51049.

Shi, Y., Ke, X., Yang, X., Liu, Y., and Hou, X. (2022). Plants response to light stress. Journal of Genetics and Genomics.

Sims, D.A., and Gamon, J.A. (2002). Relationships between leaf pigment content and spectral reflectance across a wide range of species, leaf structures and developmental stages. Remote Sensing of Environment **81**:337–354.

Sundaram, S., and Rathinasabapathi, B. (2010). Transgenic expression of fern Pteris vittata glutaredoxin PvGrx5 in Arabidopsis thaliana increases plant tolerance to high temperature stress and reduces oxidative damage to proteins. Planta **231**:361–369.

Tian, T., Liu, Y., Yan, H., You, Q., Yi, X., Du, Z., Xu, W., and Su, Z. (2017). agriGO v2. 0: a GO analysis toolkit for the agricultural community, 2017 update. Nucleic Acids Res. **45**:W122–W129.

Trapnell, C., Pachter, L., and Salzberg, S.L. (2009). TopHat: discovering splice junctions with RNA-Seq. Bioinformatics **25**:1105–1111.

Trapnell, C., Roberts, A., Goff, L., Pertea, G., Kim, D., Kelley, D.R., Pimentel, H., Salzberg, S.L., Rinn, J.L., and Pachter, L. (2012). Differential gene and transcript expression analysis of RNA-seq experiments with TopHat and Cufflinks. Nat. Protoc. **7**:562–578.

Verbon, E.H., Trapet, P.L., Stringlis, I.A., Kruijs, S., Bakker, P.A.H.M., and Pieterse, C.M.J. (2017). Iron and Immunity. Annu. Rev. Phytopathol. **55**:355–375. https://doi.org/10.1146/annurev-phyto-080516-035537.

Wada, M. (2013). Chloroplast movement. Plant Sci. **210**:177–182.

Walters, R.G. (2005). Towards an understanding of photosynthetic acclimation. J. Exp. Bot. **56**:435–447.

Wu, Q., Lin, J., Liu, J.Z., Wang, X., Lim, W., Oh, M., Park, J., Rajashekar, C., Whitham, S.A., Cheng, N.H., et al. (2012). Ectopic expression of Arabidopsis glutaredoxin AtGRXS17 enhances thermotolerance in tomato. Plant Biotechnol. J. **10**:945–955.

Yang, C.-L., Huang, Y.-T., Schmidt, W., Klein, P., Chan, M.-T., and Pan, I. (2022). Ethylene response Factor109 attunes immunity, photosynthesis, and iron homeostasis in arabidopsis leaves. Front. Plant Sci. **13**:841366.

Yu, H., Yang, J., Shi, Y., Donelson, J., Thompson, S.M., Sprague, S., Roshan, T., Wang, D.-L., Liu, J., Park, S., et al. (2017). Arabidopsis glutaredoxin S17 contributes to vegetative growth, mineral accumulation, and redox balance during iron deficiency. Front. Plant Sci. **8**:1045.

Zamioudis, C., Hanson, J., and Pieterse, C.M. (2014). β-Glucosidase BGLU42 is a MYB72-dependent key regulator of rhizobacteria-induced systemic resistance and modulates iron deficiency responses in Arabidopsis roots. New Phytol. **204**:368–379. https://doi.org/10.1111/nph.12980.

Zhang, H., Liu, P., Guo, T., Zhao, H., Bensaddek, D., Aebersold, R., and Xiong, L. (2019). Arabidopsis proteome and the mass spectral assay library. Sci. Data **6**:278.